Atmospheric Environment 276 (2022) 119021

Contents lists available at ScienceDirect

Atmospheric Environment

journal homepage: www.elsevier.com/locate/atmosenv

Stable isotopic signatures of methane from waste sources through atmospheric measurements

Semra Bakkaloglu [a,b,*], Dave Lowry [a], Rebecca E. Fisher [a], Malika Menoud [c], Mathias Lanoisellé [a], Huilin Chen [d], Thomas Röckmann [c], Euan G. Nisbet [a]

[a] Department of Earth Sciences, Royal Holloway University of London, Egham, TW20 0EX, UK
[b] Sustainable Gas Institute, Imperial College London, London, SW7 1NA, UK
[c] Institute for Marine and Atmospheric Research Utrecht, Utrecht University, Utrecht, the Netherlands
[d] Centre for Isotope Research, University of Groningen, Groningen, the Netherlands

HIGHLIGHTS

- Isotopic ^{13}C signatures from 71 waste sources in UK, NL and TR determined.
- Feedstock types have an impact on carbon isotopic signature of generated biogas.
- Open and active landfill status has a great impact on carbon isotopic signature.
- Sewage treatment is more enriched in ^{13}C than from other waste sources.
- Average $\delta^{13}C$ isotopic signature of waste sources is -55.1 ± 4.1‰.

ARTICLE INFO

Keywords:
Carbon isotopes
Deuterium
Waste isotopic signature
Methane emissions
Greenhouse gas emissions

ABSTRACT

This study aimed to characterize the carbon isotopic signatures ($\delta^{13}C$-CH_4) of several methane waste sources, predominantly in the UK, and during field campaigns in the Netherlands and Turkey. CH_4 plumes emitted from waste sources were detected during mobile surveys using a cavity ring-down spectroscopy (CRDS) analyser. Air samples were collected in the plumes for subsequent isotope analysis by gas chromatography isotope ratio mass spectrometry (GC-IRMS) to characterize $\delta^{13}C$-CH_4. The isotopic signatures were determined through a Keeling plot approach and the bivariate correlated errors and intrinsic scatter (BCES) fitting method. The $\delta^{13}C$-CH_4 and $\delta^{2}H$-CH_4 signatures were identified from biogas plants (-54.6 ± 5.6‰, n = 34; -314.4 ± 23‰ n = 3), landfills (-56.8 ± 2.3‰, n = 43; -268.2 ± 2.1‰, n = 2), sewage treatment plants (-51.6 ± 2.2‰, n = 15; -303.9 ± 22‰, n = 6), composting facilities (-54.7 ± 3.9‰, n = 6), a landfill leachate treatment plant (-57.1 ± 1.8‰, n = 2), one water treatment plant (-53.7 ± 0.1‰) and a waste recycling facility (-53.2 ± 0.2‰). The overall signature of 71 waste sources ranged from −64.4 to −44.3‰, with an average of -55.1 ± 4.1‰ (n = 102) for $\delta^{13}C$, −341 to −267‰, with an average of -300.3 ± 25‰ (n = 11) for $\delta^{2}H$, which can be distinguished from other source types in the UK such as gas leaks and ruminants. The study also demonstrates that $\delta^{2}H$-CH_4 signatures, in addition to $\delta^{13}C$-CH_4, can aid in better waste source apportionment and increase the granularity of isotope data required to improve regional modelling.

Abbreviations: BCES, Bivariate correlated errors and intrinsic scatter; CH_4, Methane; C_2H_6, Ethane; CO_2, Carbon dioxide; CRDS, Cavity ring-down spectroscopy; GC-IRMS, Gas chromatography isotope ratio mass spectrometry; GHG, Greenhouse gas; GPS, Global positioning system; H_2S, Hydrogen sulfide; IMAU, Institute for Marine and Atmospheric Research Utrecht; INSTAAR, Institute of Arctic & Alpine Research; MWe, Megawatt electric; MSW, Municipal solid waste; NAEI, National Atmospheric Emission Inventory; NL, Netherlands; NH_3, Ammonia; QGIS, Quantum Geographic Information System; TR, Turkey; UK, United Kingdom; UMEA, Ultraportable Methane-Ethane Analyser; VPDB, Vienna Pee Dee Belemnite; VSMOW, Vienna Standard Mean Ocean Water; WMO, World Meterological Organization; $\delta^{13}C$-CH_4, Carbon isotopic signature of methane; $\delta^{2}H$-CH_4, Hydrogen isotopic signature of methane.

* Corresponding author Department of Earth Sciences, Royal Holloway University of London, Egham, TW20 0EX, UK.
E-mail address: semra.bakkaloglu.2018@live.rhul.ac.uk (S. Bakkaloglu).

https://doi.org/10.1016/j.atmosenv.2022.119021
Received 14 July 2021; Received in revised form 16 February 2022; Accepted 18 February 2022
Available online 4 March 2022

1. Introduction

Methane (CH_4) is the second most significant anthropogenic greenhouse gas (GHG) after carbon dioxide (CO_2). Its global radiative forcing is 32 times greater than CO_2 over a 100-year timescale (Etminan et al., 2016), and it has a short life span (~9–10 years) compared to CO_2; therefore, reducing CH_4 emissions may produce faster climate benefits (Dlugokencky et al., 2009). Global atmospheric CH_4 mole fraction has increased over recent decades. Its growth stabilized from 1999 to 2006 but began to rise again after 2007 (Dlugokencky et al., 2009, 2011; Nisbet et al., 2019). Many studies have sought to explain variations in the recent CH_4 growth by changes in the balance between sources and sinks to better understand the global CH_4 budget (e.g., Dlugokencky et al., 2011; Rigby et al., 2017; Turner et al., 2017; Worden et al., 2017; Lan et al., 2021).

CH_4 isotope measurements ($^{12}CH_4$, $^{13}CH_4$, CH_3D) have been widely used to investigate changes in the global CH_4 growth rate and determine the relative contributions of individual emission sources (Beck et al., 2012; France et al., 2016; Levin et al., 1993; Lowry et al., 2001, 2020; Monteil et al., 2011; Nisbet et al., 2016; Rice et al., 2016; Schaefer et al., 2016; Townsend-Small et al., 2012, 2014; Zazzeri et al., 2015). The stable isotopic ratios of CH_4 differ according to the origin and generation processes of the CH_4. Thermogenic (e.g. fossil fuel), pyrogenic (e.g. biomass burning, incomplete combustion) and biogenic (e.g. waste, agricultural and wetland) sources have distinct isotopic signatures, although there is some overlap between categories that does not always allow conclusive source attribution (e.g. Lassey et al., 2011; Menoud et al., 2020a; Milkov and Etiope, 2018; Sherwood et al., 2017). Pyrogenic and thermogenic CH_4 sources are generally relatively enriched in ^{13}C and deuterium (D, ^2H), with values of $\delta^{13}C\text{-}CH_4$ from −30 to −12.5‰ reported on the Vienna Pee Dee Belemnite (VPDB) scale and $\delta^2H\text{-}CH_4$ values of −232 to −195‰ reported on the Vienna Standard Mean Ocean Water (VSMOW) scale for the pyrogenic sources (Quay et al., 1999; Sherwood et al., 2017), and $\delta^{13}C\text{-}CH_4$ from −45 to −15‰ and $\delta^2H\text{-}CH_4$ from −350 to −100‰ for the thermogenic sources (Milkov and Etiope, 2018; Sherwood et al., 2017). Previous studies demonstrate that $\delta^2H\text{-}CH_4$ may provide better information to distinguish between fossil fuels and biological sources, if the fossil fuels are depleted in ^{13}C relative to atmospheric background (Sherwood et al., 2017; Townsend-Small et al., 2012, 2016). CH_4 from biogenic sources is more depleted in ^{13}C and ^2H with respect to the pyrogenic and thermogenic sources, with $\delta^{13}C\text{-}CH_4$ ranging from −90 to −45‰ and $\delta^2H\text{-}CH_4$ from −450 to −125‰, owing to the fractionation that occurs during anaerobic fermentation of organic matter or CO_2 reduction (e.g., Bergamaschi et al., 1998; Levin et al., 1999, 1993; Lopez et al., 2017; Lowry et al., 2020; Milkov and Etiope, 2018; Quay et al., 1988; Sherwood et al., 2017; Xueref-Remy et al., 2020; Zazzeri et al., 2015). The methanogenic pathway also influences the fractionation factor, which is affected by a range of parameters such as microbial community type and population, pH, nutrient amount, ratio of CH_4/O_2, environment temperature, presence of inhibiting chemicals and inorganic nitrogen (Bakkaloglu et al., 2021b; Templeton et al., 2006); therefore, bacterial oxidation of CH_4 at varying rates produces isotopic enrichment and a positive correlation between isotopes of ^{13}C and ^2H (Whiticar, 1999). For instance, CH_4 from acetate fermentation ($\delta^{13}C\text{-}CH_4 = -90$ to −45‰; $\delta^2H\text{-}CH_4 = -450$ to −250‰) is more enriched in ^{13}C and less enriched in ^2H than CH_4 from CO_2 reduction ($\delta^{13}C\text{-}CH_4 = -90$ to −60‰; $\delta^2H\text{-}CH_4 = -350$ to −125‰) (Milkov and Etiope, 2018).

Isotope ratio data are widely used in atmospheric models to understand the individual contributions of various CH_4 sources in the CH_4 budget at a global or regional scale (e.g., Bousquet et al., 2006; Menoud et al., 2020a; b; Quay et al., 1991; Röckmann et al., 2016). The $\delta^{13}C\text{-}CH_4$ of atmospheric CH_4 has shifted to more negative values since 2007, coinciding with a sharp increase in the CH_4 mole fraction following period of slow growth between 1999 and 2006 (Nisbet et al., 2019, 2021; Schaefer et al., 2016). However, the reason for this negative shift remains a topic of debate, and there is considerable uncertainty about source isotopic signatures owing to large temporal variabilities and regional specificities (e.g., Sherwood et al., 2017). These uncertainties can be minimized significantly by focusing on a regional scale.

This study sought to identify various waste source signatures, primarily in the UK, and during campaigns in the Netherlands and Turkey, and link them with particular processes using isotope ratio characterisation so as to assess the current and evolving waste treatment sources. Waste management practices have changed in recent years, linked with the move away from landfill waste disposal toward biogas production, composting and the general trend toward recycling. CH_4 emissions from waste sources account for approximately 12% of total global anthropogenic emissions (Saunois et al., 2020), and are the second largest source of anthropogenic CH_4 emissions into the atmosphere, accounting for nearly 37% of CH_4 emissions in the UK (NAEI, 2022) and around 23% in Europe (EEA, 2020). Based on the Net Zero Technical Report (CCC, 2019), the UK government targets to reduce GHG emissions to net zero by 2050. For this purpose, it has been recommended that sending biodegradable waste to landfill should be banned from 2025 (CCC, 2019). Literature values for the isotopic signatures of waste CH_4 range from −74 to −40‰ (see Table 1). Recent compilations of the $\delta^{13}C$ signature of landfill and sewage emissions have suggested that the average signatures are between −57 and −55‰ (Dlugokencky et al., 2011; Monteil et al., 2011; Sherwood et al., 2017). There have been a small number of studies measuring waste δ^2H with a range of signatures between −312 and −281‰ (Schoell, 1980; Sherwood et al., 2017; Townsend-Small et al., 2012, 2016). Previous studies also show that types of waste and treatment processes may impact significantly the isotopic signatures (Yang et al., 2019).

According to the UK Net-Zero Commitment (CCC, 2019), more material is recycled, and biodegradable waste should be diverted from landfills to anaerobic digesters and composting facilities. As a result, variations in waste practices are expected to have an impact on their isotopic signatures when compared to previous reporting. In particular, the isotopic signatures of biogas plant emissions have not yet been studied in detail as they are a recent innovation in the UK, and recent databases of isotopic signatures of major CH_4 sources are mainly based on North American fossil fuel sources rather than waste sources (Milkov and Etiope, 2018; Sherwood et al., 2017). Thus, new studies of the signatures of each waste source category are required to improve the isotopic data supporting regional or global source attribution modelling, as well as to understand the evolution of waste source isotopic signatures.

In this study, different potential waste sources were surveyed using CRDS instruments in a vehicle to identify plumes of CH_4 for sampling and subsequent high precision GC-IRMS measurement. Keeling plot analysis was used to investigate variations between different waste sources. Selected samples were also analysed for $\delta^2H\text{-}CH_4$. The source category signatures were evaluated to observe if they could be separated from signatures of other source categories emitting to atmosphere based on isotopic signatures alone. During 39 mobile measurement days between 2018 and 2020, emission plumes from 26 biogas plants, 27 landfills, 11 sewage treatment plants, one water treatment plant, four composting facilities, one landfill leachate treatment plant and a waste recycling facility were measured to provide a better estimation of the contribution of each waste source to emission inventories for utilization in regional and global scale modelling.

2. Materials and methods

2.1. Study sites

The campaigns were conducted in England and the Netherlands between 2018 and 2020 to identify potential waste sources. Prior to each campaign, waste source locations were determined from national inventory and Google Earth maps. In most cases, the UK's National

Table 1
Stable isotopic ratios of CH_4 waste emissions from previous studies.

Location	Source	δ^{13}C-CH_4 (‰, VPDB)	δ^{2}H-CH_4 (‰, VSMOW)	References
UK	Landfill	−64 to −54	−308 to −233	Hitchman et al. (1990)
UK	Sewage	−51.6	−265	Hitchman et al. (1990)
UK	Anaerobic digester	−74.4 to −48.4	−342 to −286	Hitchman et al. (1990)
Germany	Landfill	−62.9 to −52	−312 ± 8	Levin et al. (1993)
Germany	Biogas generator	−51.8 ± 2.8	−305 ± 12	Levin et al. (1993)
Germany	Waste	−55.4 ± 1.4		Levin et al. (1999)
Different locations	Landfill	−50 ± 2	−310 ± 10	Quay et al. (1999)
Various sites in Europe	Landfill	−55.4 ± 1.4		Bergamaschi et al. (1998)
US	Landfill	−48.1 to −50.4	−273 to −281	Liptay et al. (1998)
UK	Landfill	−52.6 to −50.8		Lowry et al. (2001)
Sweden	Active landfill	−52.9 to −58.1		Börjesson et al. (2007)
Sweden	Closed landfill	−52.2 to −50.3		Börjesson et al. (2007)
Global	Landfills/waste	−55		Monteil et al. (2011)
Japan	Sewage treatment (different stages)	−45.5 to −51.7		Toyoda et al. (2011)
Los Angeles, US	Sewage treatment	−47 to −46.3	−298	Townsend-Small et al. (2012)
Los Angeles, US	Landfill gas collection	−61.9 to −61.5	−316.1 to −313.9	Townsend-Small et al. (2012)
Riverside County, US	Manure digestor test facility	−52.4 to −50.2	−333.6 to −280	Townsend-Small et al. (2012)
Boston, US	Biogenic sources	−64.5 to −53.1		Phillips et al. (2013)
UK	Sewage treatment	−59.2 to −48.1		Zazzeri et al. (2015)
UK	Active landfill	−59.7 to −55.2		Zazzeri et al. (2015)
Germany	Anaerobic digester	−60 to −40		Polag et al. (2015)
Colorado, US	Active Landfill	−58.1 ± 1.4	−290 ± 4	Townsend-Small et al. (2016)
Canada	Landfill	−55.3 ± 0.2		Lopez et al. (2017)
Global	Waste	−73.9 to −45.5	−312 to −281	Sherwood et al. (2017)
Germany	Landfill	−62.2 to −54.2		Hoheisel et al. (2019)
Germany	Biogas	−64.2 to −59.0		Hoheisel et al. (2019)
Germany	Sewage treatment	−51.3 ± 0.2		Hoheisel et al. (2019)
France	Sewage treatment	−55.3 to −51.0		Xueref-Remy et al. (2020)
France	Landfill	−65.9 to −53.0		Xueref-Remy et al. (2020)
Houston, US	McCarty landfill	−61.8 to −54.4		Yang et al. (2019)
Houston, US	Greenbelt landfill	−60.5 to −56.8		Yang et al. (2019)
Houston, US	Houston solid waste management	−53 to −46.9		Yang et al. (2019)
UK	Active landfills	−61 to −56		Lowry et al. (2020)
UK	Closed landfills			Lowry et al. (2020)
		−58 to −53		
Kuwait	Active landfill	−59.5 to −58.5		Al-Shalan et al. (2022)
Kuwait	Closed landfill	−56.4 to −51.9		Al-Shalan et al. (2022)
Kuwait	Sewage Treatment	−59.2 to −45.1		Al-Shalan et al. (2022)

Atmospheric Emissions Inventory (NAEI, 2022) website (http://naei.defra.gov.uk/) was used to determine potential CH_4 emissions based on the most recent inventory, 2019. However, as most UK biogas plants are not included in NAEI point source data, they were assessed from the official information portal on anaerobic digestion (http://www.biogas-info.co.uk/; NNFCC, 2022).

We surveyed plume transects as close as possible downwind of the source. CH_4 plumes were detected while driving downwind of sources on public roads. Once a CH_4 plume was detected at a source location, downwind ambient air samples were collected for further δ^{13}C-CH_4 analysis. The downwind air samples from landfill and sewage treatment plants in Turkey were collected without the use of mobile measurement equipment (see Fig. 1 for locations).

2.1.1. Biogas plants

Biogas plants rely on anaerobic digestion, which is breakdown of the organic material by microorganisms under anaerobic conditions. Biogas plants can be fed any type of biodegradable materials called feedstock such as manure, food waste, maize, sludge and energy crops to produce biogas that contains CH_4 (50–70%), CO_2 (30–50%) and trace gases (H_2S and NH_3) (UNFCCC, 2017). Biogas can be utilised to generate either heat or electricity or both. It can also be converted to biomethane and injected into the gas grid as well as used as transportation fuel (NNFCC, 2021). The size of the biogas plants is determined by the amount of annual feedstock used (tonne yr^{-1}) in relation to the amount of power generated (MWe), and biomethane produced ($Nm^3\ h^{-1}$). According to NAEI, anaerobic digesters in the UK emitted 8.5 kilotonnes of CH_4 in 2019 (NAEI, 2022), making them the second-lowest emissions source in the waste sector after incineration, despite recent studies indicating that they could be much higher than inventory suggests (Bakkaloglu et al., 2021a).

A total of 26 biogas plants – five in the Netherlands and 19 in the UK – were investigated during the mobile campaigns. The various feedstock materials were taken into consideration in selecting the plants. We also aimed to examine the feedstock materials' impact on stable isotopic signatures. The biogas plants comprised nine food waste, six municipal solid waste, four maize, two sugar beet, one papermill, and four mixed type such as animal slurry, maize, and grass silage-fed plants. Some were surveyed more than once to quantify their emission rates (see Bakkaloglu et al., 2021a.). The survey dates, number of samples collected and excess CH_4 mole fractions with stable isotope signatures are given in the supplementary information (S1).

2.1.2. Landfill sites

Landfills are the primary source of CH_4 in the UK waste sector. They were estimated to emit 574 kilotonnes of CH_4 in 2019 (NAEI, 2022). Twenty-seven different landfills were investigated (UK - 23, Netherlands - 3, Turkey - 1). Five landfill sites had both active and closed areas, and one landfill was surveyed while it was accepting waste and again after it was closed, totalling 20 active and 12 closed sites plumes sampled. Nearly all active sites have older closed areas as well. All sites have an operating gas extraction system, that collects CH_4-rich landfill gas for combustion or supply to the distribution grid as green gas. Isotopic

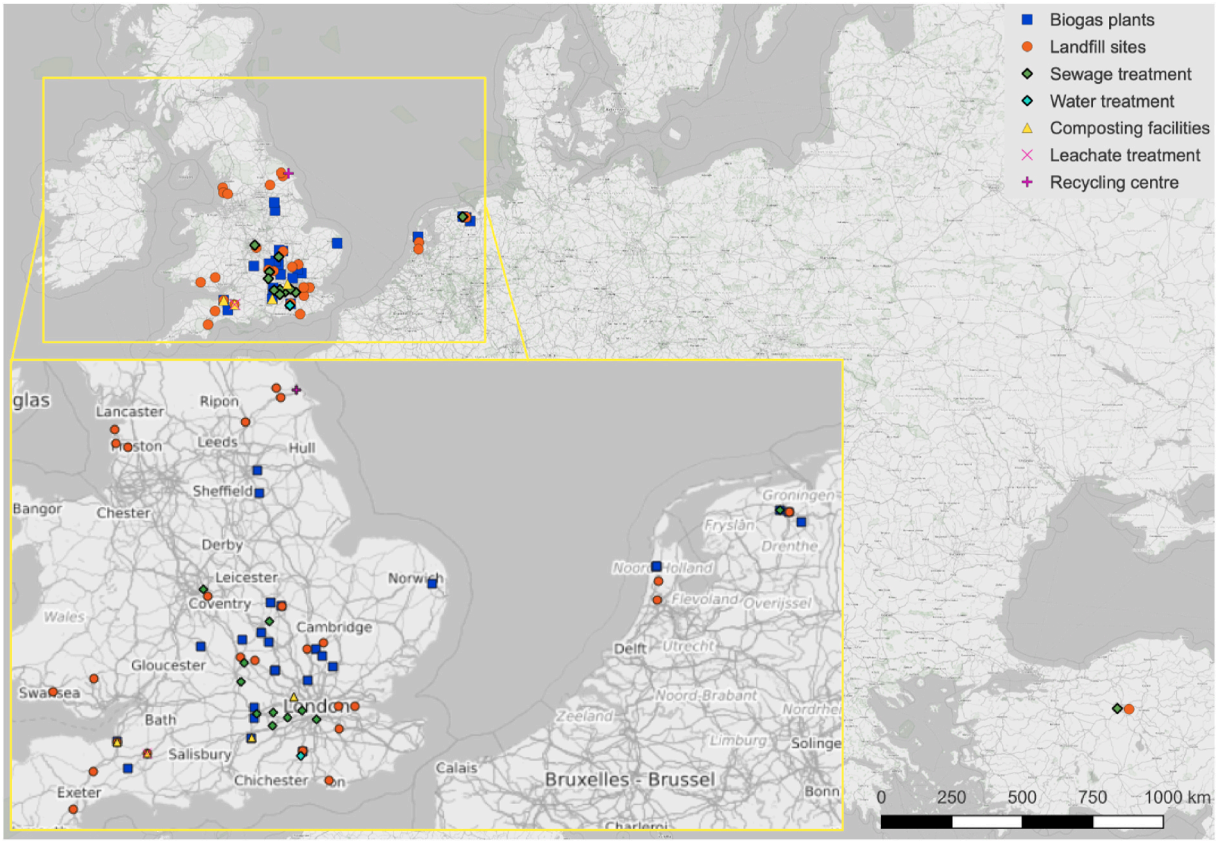

Fig. 1. The map for locations and categories of sampling sites created using QGIS software (QGIS Development Team, 2021). Some source points overlap due to close proximity (see supplementary information S1; S2; S3; S4 for details).

signatures of landfill sites are given in the supplementary information (S2).

2.1.3. Sewage and waste treatment plants

Sewage treatment plants treat the wastewater before discharging it into a water body such as lake, river or sea; on the other hand, water treatment plants remove the contaminants before it is used or drunk. As a result, the inflow of sewage treatment plants has a much higher organic load than that of water treatment plants, which will affect the emissions from the treatment plants. Sewage treatments are the UK's second largest waste source of CH_4 emissions, accounting for 67.2 kilotonnes of CH4 emissions in 2019 (NAEI, 2022).

Emission plumes from 11 sewage treatment plants were surveyed in the UK (9), the Netherlands (1), and Turkey (1). A CH_4 plume was also observed at one UK water treatment plant. A list of these is given in the supplementary information (S3).

2.1.4. Composting facilities and leachate treatment plants

Four composting sites in the UK and one UK leachate treatment plant were surveyed, as detailed in the supplementary information (S4). One UK waste recycling facility was also surveyed. Composting plants were estimated to emit 40.9 kilotonnes of CH_4 in 2019, ranking them third among waste CH_4 sources.

2.2. Air sampling methodology

A Picarro G2301-m (CO_2, CH_4 and H_2O, measuring each 3 s) cavity ring-down spectroscopy (CRDS) analyser, a GPS sensor (every 1 s) and an air inlet line were used for sampling during the UK mobile campaigns (for details, see Zazzeri et al., 2015; Lowry et al., 2020). The vehicle used in the UK was a small sport utility vehicle. The air inlet was at 1.8 m height above ground and approximately 20 cm above the roof of the vehicle. When a large elevation of CH_4 (above than the background mole fraction) was observed, the vehicle was stopped at a safe location to sample the plume. The excess CH_4 over background measured off site ranged from 0.1 to 19 ppm depending on the plume source, with landfill plumes having a higher mole fraction than other waste sources (see supplementary information for details). Air samples were collected in three- or 5-L Flexfoil bags (SKC Ltd) using a small battery-operated KNF diaphragm pump, with sufficient air to analyse both the mole fraction (1 L) and isotope signature analysis (all for $\delta^{13}C$, selected for $\delta^{2}H$ - 0.6 L in total). This used a separate sample inlet adjacent to the instrument lines on the vehicle roof. This was flushed with air at the beginning of each air sample collection process to avoid mixing of residual air from the previous sample. We aimed to fill the bag with a range of CH_4 mole fractions to allow more precise isotopic signature characterisation (see more details in Lowry et al., 2020). The background air was typically collected from upwind of the sources at the beginning or end of the campaign, or close to each sampled large plume if the CH_4 background mole fraction was continuously decreasing during atmospheric inversion break-up.

The locations of waste sources in the UK were determined using the NAEI's (2022) map of CH_4 emissions for UK landfills and sewage treatment plants as well as Google Earth map. Routes were planned prior to each campaign so that key source targets close to each other and/or our base in SE England were surveyed on the same day, taking into consideration the closest public roads and prevailing wind direction. A few sources were very close to each other, which necessitated separation of the plumes by considering the very specific wind direction at a constant speed with low turbulence. During the survey, we kept track of the plume peaks and separated them according to the downwind sampling location and the wind direction perpendicular to the source. We also attempted to collect air samples closer to some sources on foot, mainly at landfill sites where landfill, composting and leachate treatments were sometimes adjacent to each other. Moreover, we monitored the plumes

using an additional instrument, a Los Gatos Research UMEA (Ultra-portable Methane-Ethane Analyser) which allowed us to distinguish between the peak of a natural gas leak coming from distribution pipelines and waste sources because the UMEA measures ethane (C_2H_6), which is present in natural gas.

2.3. Laboratory analysis

The CH_4 mole fraction of the air samples collected were analysed at Royal Holloway's GHG laboratory using a Picarro G1301 CRDS analyser with a precision of ±0.3 ppb, calibrated weekly to the WMO X2004A scale (for details, see Zazzeri et al., 2015). The remaining samples were then measured for δ^{13}C-CH_4, utilizing continuous-flow gas chromatography/isotope-ratio mass spectrometry (GC-IRMS) with a high-precision (short -term reproducibility 0.05‰, 1σ) modified Trace Gas–IsoPrime system as described in Fisher et al. (2006). The isotope ratios were expressed in δ-notation relative to the VPDB standard in parts per thousand (‰).

At the beginning of each day and after every two samples, an internal secondary standard reference gas was analysed to correct for occasional instrumental drift throughout the day. The internal standards are assigned signatures based on comparison with measurements of air cylinders that have also been analysed by the INSTAAR laboratory (see Umezawa et al., 2018 for details of differences in δ^{13}C-CH_4 measurements between laboratories). Each collected air sample was measured at least three times to improve precision. Samples with CH_4 mole fractions higher than seven parts per million (ppm) were diluted with high-purity N_2 to meet the linear range of the mass spectrometer for isotopic analysis (for details of instrument calibration see Fisher et al., 2006; for details of mobile campaign data correction see Zazzeri et al., 2015).

In addition, a subset of samples from the main waste source categories were sent to IMAU, Utrecht University, to be analysed for δ^2H in CH_4, using a Thermo Scientific Delta plus XL IRMS coupled to a sample preparation system with reproducibility better than 2‰ (for further details of this method, see Brass and Röckmann, 2010; Röckmann et al., 2016). The isotope ratios were expressed in δ-notation relative to the VSMOW standard.

2.4. Isotopic source signatures and data processing

Keeling plot analysis (Keeling, 1958; Zazzeri et al., 2017; Pataki et al., 2003) was used to identify the isotopic source signatures of the CH_4 in the air bag samples. The δ^{13}C-CH_4 and δ^2H-CH_4 were plotted against the inverse of CH_4 mole fraction (see Supplementary Information Figs. S1) and a linear regression was then applied to calculate the isotopic source signature responsible for the excess over background (Equation (1)), which is unique for each measurement. The y-intercepts gave the isotopic signatures of the sources.

$$\delta^{13}C_a = C_b\,(\delta^{13}C_b - \delta^{13}C_s)\ x\ (1/C_a) + \delta^{13}C_s \qquad \text{(Equation 1)}$$

where C_a is the atmospheric mole fraction of a gas, C_b is the background atmospheric mole fraction, $\delta^{13}C_a$ is the measured isotopic composition, $\delta^{13}C_b$ is the background isotopic composition and $\delta^{13}C_s$ is the source isotopic composition.

To assess errors in the calculation of both x and y variables, a bivariate correlated errors and intrinsic scatter (BCES) code was used for each sample. BCES regression accounts for correlated errors between CH_4^{-1} and δ^{13}C (δ^2H) and calculates the uncertainty of the slope and Keeling plot intercept (Akritas and Bershady, 1996; Zazzeri et al., 2015). Several previous studies (Xueref-Remy et al., 2020; Zazzeri et al., 2016, 2017) have used this technique (for further details, see France et al., 2016; Zazzeri et al., 2015).

3. Results and discussion

3.1. Isotopic signatures of biogas plants

In this study, the δ^{13}C-CH_4 values ranged from −64.4 to −44.3‰, with an average of −54.6 ± 5.6‰ (see Fig. 2 and supplementary information S2). The majority (82%) of the δ^{13}C-CH_4 values fall between −64.4 and −50.5‰, with an average of −56.4‰. These results are slightly more enriched in ^{13}C than Hoheisel et al.'s (2019) results of −61.5 ± 0.1‰ and −64.1 ± 0.3‰ for maize-silage and food waste tanks, respectively (see Table 1). In this study, the most enriched values came from maize-fed biogas plants (see Fig. 3). CH_4 from agricultural maize-waste biogas plants fed with more than 50% maize had more enriched signatures, with an average of −45.7 ± 1.4‰. Because maize is a C4 crop and is 10–15‰ more enriched in ^{13}C than typical C3 vegetation (Levin et al., 1993), the average isotopic signature for CH_4 produced by agricultural biogas plants that use this feedstock shifted toward ^{13}C-enrichment. Papermill-waste (C3 trees) biogas plants had more depleted signatures than other types of biogas plants (see Fig. 3).

Food-waste biogas plants including sugar beet and the organic fraction of municipal solid waste (MSW) plants emitted CH_4 with larger isotope ranges compared to other feedstocks (Fig. 3). This large variability in the δ^{13}C values indicates that methanogenic pathways, the source of substrate, operating temperature, moisture, pH and type of bacteria may differ according to the type of feedstock, causing changes in carbon isotope value.

In biogas plants, methanogenesis produces CH_4 under anaerobic conditions through various metabolic pathways. The isotopic signature of CH_4 in anaerobic digesters depends on the substrate types and loading rates, the quantity and activity of the methanogenic community, and operational conditions such as temperature, acidity (pH) and hydraulic retention times (Polag et al., 2015). Similarly, our findings demonstrate that the different biogas plant feedstocks produce distinctive isotopic signatures (see Fig. 3).

3.2. Isotopic signature of landfills

The isotopic signatures of CH_4 from landfills ranged from −62 to −52‰, with an average of −56.8 ± 2.3‰ (see Fig. 4 and supplementary information S2). The active landfill sites (with an averaged value of −57.8 ± 2.1‰) emitted CH_4 that was more depleted in ^{13}C than the closed landfill sites (with an average value of −54.9 ± 1.4‰) (see Fig. 5) owing to the soil cover (Bakkaloglu et al., 2021b). CH_4 escapes directly

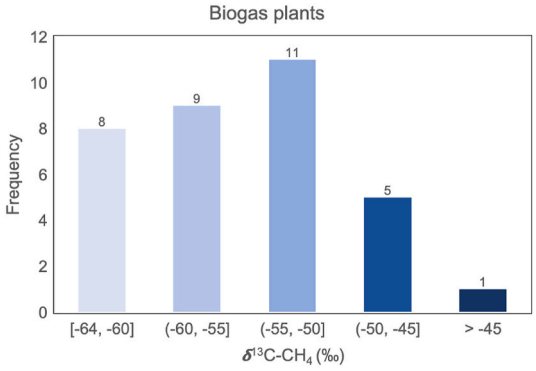

Fig. 2. Isotopic signature distribution of biogas plants. The colours of the bars show the different carbon isotopic signature categories (indicated on the x axis) with the number of data points at the top of each column. The average source signature for the 34 plumes measured from the 26 sites is −54.6 ± 5.6‰, with a median value of −54.2‰. Some sites were surveyed more than once. (See the Supplementary information, S1 for details.). (For interpretation of the references to colour in this figure legend, the reader is referred to the Web version of this article.)

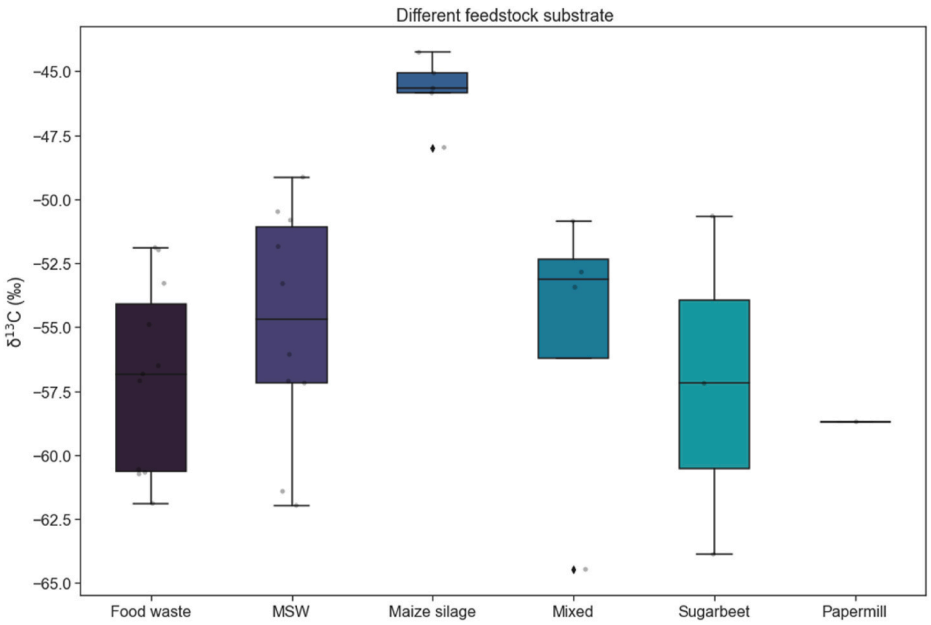

Fig. 3. Isotopic signature variations between the UK biogas plants relating to different feedstock substrate material, such as food waste (n = 11), municipal solid waste (MSW, n = 10), maize silage (n = 5), mixed (n = 4), sugar beet (n = 3) and papermill (n = 1). The figure shows the mean line, interquartile calculation includes median value. Mixed included the agricultural slurry, maize, and grass silage.

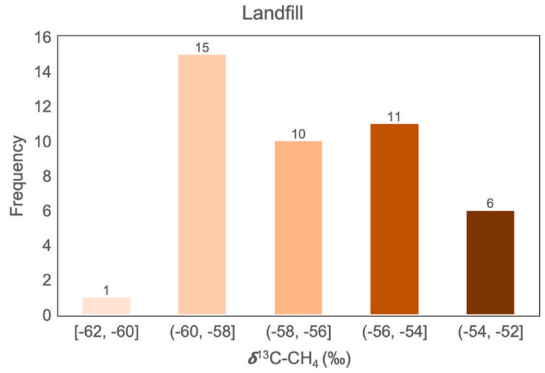

Fig. 4. Isotopic signature distribution of CH_4 emitted from landfills. The colours of the bars show the different carbon isotopic signature categories with the number of data points at the top of each column. The average source signature for the 43 plumes measured from the 27 sites is −56.8 ± 2.3‰, with a median value of −57.2‰. Some sites were surveyed more than once. (See the Supplementary information, S2 for details.). (For interpretation of the references to colour in this figure legend, the reader is referred to the Web version of this article.)

to the atmosphere from operational cells of active landfill sites because they do not have topsoil cover. Furthermore, aerobic bacteria in the soil cover oxidise CH_4 generated in the landfill, causing a shift to more enriched isotopic signatures for CH_4 emitted into the atmosphere from closed landfill cells (Bakkaloglu et al., 2021b). The isotopic signatures of CH_4 from landfills may vary with waste composition, temperature and the methanotrophic top-soil oxidation rate (Liptay et al., 1998).

Four landfills (LA4, LA5, LA6 and LA11 see supplementary information S2) had previously been surveyed in 2013 by Zazzeri et al. (2015). All of our results, approximately five years later, showed that the emitted CH_4 was more enriched in ^{13}C, with differences of 0.6–4.7‰ between our results and theirs. This could be due to changes in the concentration of organic matter and the age of the landfills, because less available substrate causes ^{13}C- enriched CH_4 to be released (Bakkaloglu et al., 2021b). The CH_4 mole fractions measured downwind of landfills LA4 and LA5 were around 4 ppm lower than those reported in Zazzeri et al. (2015). The reduction in the excess CH_4 mole fraction is expected as a result of the current closure of the sites but could also be related to different meteorological conditions on the different survey days.

The average carbon isotopic signature of CH_4 from active landfills from the UK (15), the Netherlands (3), and Turkey (1) were recorded as −58.5 ± 1.3‰, −55.5 ± 2.8‰ and −55.8 ± 0.8‰, respectively. In Fig. 5, additional waste source signature values from the Netherlands, Germany, France and Poland were added into this study results from Menoud et al. (2020). The overall landfill $\delta^{13}C$-CH_4 signatures are similar for these countries (see Fig. 5) although the active landfill isotopic signatures reveal a wider range than closed landfills. The greater variation in active landfill isotopic signature may be due to different regulations in those countries as well as diverse waste materials actively placed over a variety of timeframes.

3.3. Sewage and water treatment plants

The isotopic signatures of CH_4 from sewage treatment plants ranged from −56.8 to −47.8‰, with an average of −51.6 ± 2.2‰ (see Fig. 6). These results are comparable with those of Hoheisel et al. (2019), Xueref-Remy et al. (2020) and Toyoda et al. (2011).

Toyoda et al. (2011) show that different stages of sewage treatment produce CH_4 with different isotopic signatures. For instance, CH_4 from an aeration tank was more enriched in ^{13}C (−45.5‰) than a secondary settling tank (−51.7‰). Because we were interested in the overall signature emissions from sewage plants to atmosphere in this study and we had no access to the inside of sewage treatment facilities, we were unable to distinguish the isotopic signatures of each step of the treatment process. However, the results can indicate that sludge treatment processes such as anaerobic digestion leads to greater depletion of ^{13}C than aerobic treatment. It should be noted also that CH_4 emissions from sewage plants highly depend on dissolved oxygen concentration in aeration basins and water temperature in high density clarifiers (Wang et al., 2011).

A CH_4 downwind plume was detected outside of one of the water treatment facilities surveyed. The water treatment process mainly involves the treatment of raw water such as river water to produce a standardised end-use product like drinking water. The CH_4 emissions

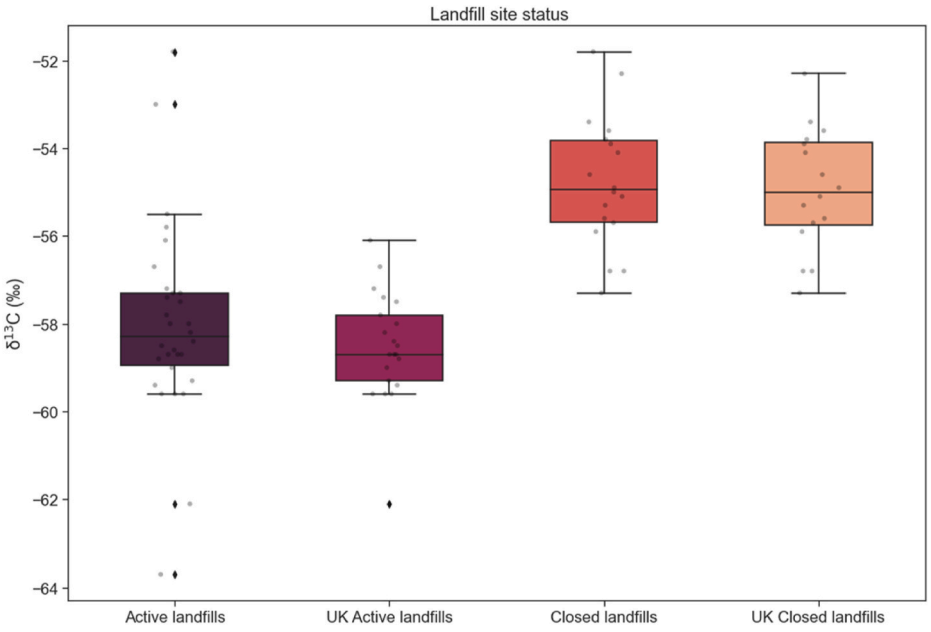

Fig. 5. Isotopic signature distribution differences between CH_4 emitted from active and closed landfills. Additional data from the MEMO^2 database (Menoud et al., 2020) were added to current active landfill data. These were from the Netherlands (3), France (2), Germany (1). Closed landfills included one additional data point from Poland and one from the Netherlands (Menoud et al., 2020). The mean and median isotopic signature of CH_4 from the all active and closed landfills studied are −58.0 ± 2.3‰ and −58.3‰, −54.8 ± 1.5‰ and −55.0‰, respectively. UK active landfills have −58.5 ± 1.3‰ mean and −58.7‰ median values, UK closed landfills have −54.9 ± 1.4‰ mean and −55.0‰ median values.

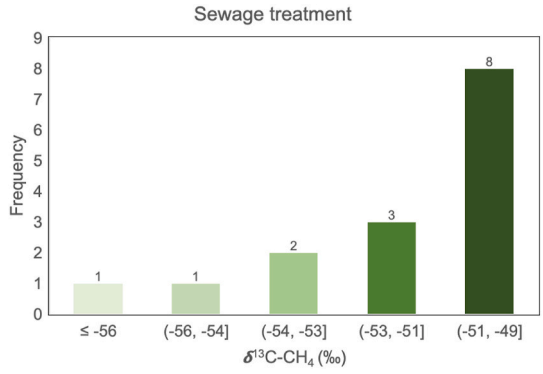

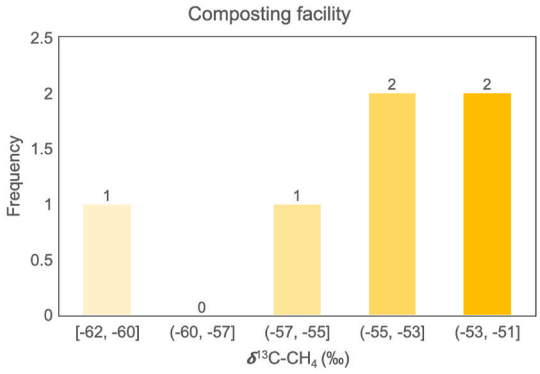

Fig. 6. Isotopic signature distribution of CH_4 from sewage treatment. The colours of the bars show the different carbon isotopic signature categories with the number of data points at the top of each column. The average source signature for the 15 plumes measured from the 11 sites −51.6 ± 2.2‰, with a median value of −51.1‰. Some sites were surveyed more than once. (See the Supplementary information, S3 for details.). (For interpretation of the references to colour in this figure legend, the reader is referred to the Web version of this article.)

Fig. 7. Isotopic signature distribution of CH_4 from composting facilities measured in this study. The colours of the bars show the different carbon isotopic signature categories with the number of data points at the top of each column. The average source signature for the 6 plumes measured from the 4 sites is −54.7 ± 3.9‰, with a median value of −54.1‰. Some sites were surveyed more than once (See the Supplementary information, S4 for details). (For interpretation of the references to colour in this figure legend, the reader is referred to the Web version of this article.)

from the water treatment had a δ^{13}C-CH_4 signature of −53.7 ± 0.1‰, which is more depleted in ^{13}C compared to the downwind plume coming from a raw water pond (Lu et al., 2021).

3.4. Composting facilities and leachate treatment

The four composting facilities and one leachate treatment plant in the UK surveyed in this study are listed in the supplementary information five (S5), together with the δ^{13}C signatures of the plumes sampled. The isotopic signatures of the CH_4 from composting facilities ranged from −62 to −51‰, with an average of −54.7 ± 3.9‰ (Fig. 7). This wide isotopic range might be due to the process of how frequently waste is aerated and new waste is loaded, also the frequency of waterlogging leading back to anaerobic conditions.

Because most of the composting facilities were in close proximity to other waste sources such as landfill, biogas plants and even farms, it was very challenging to characterize their isotopic signatures. But we managed to obtain six plumes from the four different composting facilities as seen in Fig. 7. Two of these facilities were surveyed twice on separate days (see Supplementary Information Table S4 for details).

One leachate treatment plant at a landfill site produced CH_4 with δ^{13}C signatures that varied between −58.3 ± 0.5‰ in summer and −55.8 ± 0.1‰ in winter. While there are limited number of air samples from leachate treatment plants, these differences were likely due to temperature changes between the two surveys (see supplementary information S4). As microbial degradation is highly dependent on temperature, the colder weather conditions result in more enrichment in ^{13}C.

3.5. Overall waste sources

δ^{13}C values for CH_4 emitted from all waste sources measured in this study ranged from −64 to −44‰ (n = 102), with an unweighted average of −55.1 ± 4.1‰ (see Fig. 8), and δ^2H-CH_4 values from 11 different sources ranged between −341 and −267‰, with an unweighted average of −300.3 ± 25‰ (see Fig. 9). These new source isotopic signature

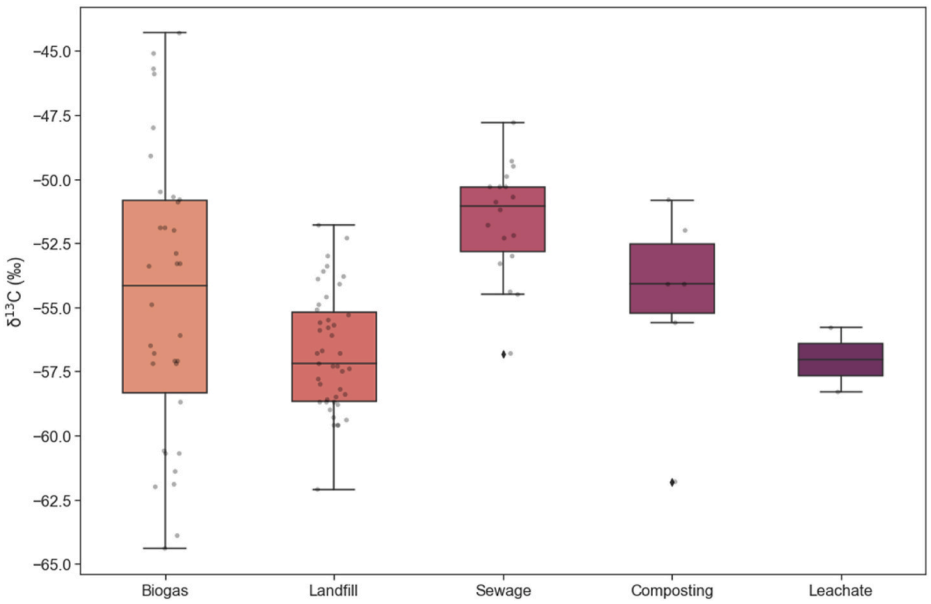

Fig. 8. Isotopic signature distribution of CH_4 for European waste sources: biogas (n = 34), landfill (n = 43), sewage (n = 15), composting (n = 6) and leachate (n = 2). Additional data were included from MEMO^2 database (Menoud et al., 2020).

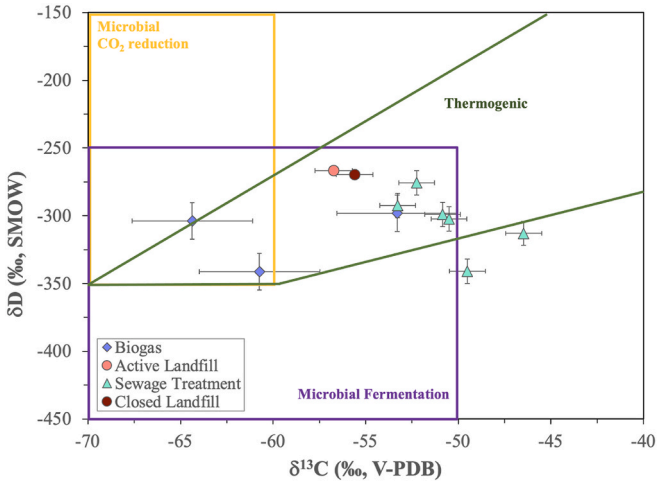

Fig. 9. δ^2H vs δ^{13}C of CH_4 from waste sources mainly in the UK and one sewage plant in the Netherlands, measured in this study. The background boxes demonstrate the previous studies range of values (Milkov and Etiope, 2018; Sherwood et al., 2017; Whiticar, 1999; 1990). The global average atmospheric δ^{13}C of CH_4 was −47.3‰ for the year 2016 (White et al., 2017) and −95.5‰ for δ^2H in the year 2015 (Sherwood et al., 2017).

results are in line with Sherwood et al. (2017) who reported the mean values of global waste δ^{13}C and δ^2H as −56‰ and −298‰, respectively. Monteil et al. (2011) also evaluated previous measurements and suggested a value of $\delta^{13}C = -55‰$ to represent a global average for CH_4 from landfills/waste, which is in good agreement with our result. Levin et al. (1993) reported −55.4 ± 1.4‰ for the δ^{13}C-CH_4 value of waste, which is also similar to this study. Yang et al. (2019) described the solid waste management carbon isotopic signature as −53 to −43.9‰, which is a slightly more ^{13}C-enriched range. These differences can be attributed to variations in the waste source substance. When the estimated inventory emission of the UK waste sources for 2019 is taken into account, the weighted average δ^{13}C and δ^2H for waste sources are −56.1 ± 2.4‰ and −272.5 ± 4.2‰, respectively (see Supplementary Table S5 for details). As the landfill emissions are reduced and biogas and composting plant utilization is increased due to Net-Zero targets, the isotopic signature of waste sources is predicted to be more enriched in ^{13}C and more depleted in ^{2}H in coming years.

CH_4 from the biogas plants had a wider range of isotopic signatures than other waste sources. This difference may have been due to the variety of feedstock materials, particularly maize, as well as the higher number of air samples collected compared to other waste sources. Although all the CH_4 waste-source isotopic signatures originated from biogenic sources, sewage treatment clearly produced the highest enrichments in ^{13}C, at around −50‰ compared with other sources. This reason may be due to aeration in an activated sludge process in the wastewater treatment plants. Our enriched ^{13}C sewage treatment results are in general agreement with Townsend-Small et al. (2012) and Toyoda et al. (2011) (see Table 1).

3.6. Comparison of deuterium and carbon isotopic signatures

Fig. 9 demonstrates that the isotopic composition of CH_4 emitted from waste related sources spans a large range, which does not precisely fall into the microbial fermentation category. Biogas plant CH_4 emissions have similar δ^2H signatures compared to other waste sources. Their methanogenic pathway overlaps with both microbial CO_2 reduction (Milkov and Etiope, 2018) and microbial fermentation. The isotopic signatures of landfill and sewage are generally in the range that was previously reported for the microbial fermentation pathway, but some sewage treatment samples were more enriched in ^{13}C, and the active landfill samples were slightly more enriched in ^{2}H. The deuterium isotopic signatures observed for CH_4 from three UK biogas plants (Fig. 9) range from −341.3 to −298.2‰, with an averaged value of −314.4 ± 23‰ (see Supplementary information S1, for details). In the literature, Levin et al. (1993) only reported one biogas generator deuterium signature for four samples as −305 ± 49‰, which is in line with our findings when the uncertainty ranges are considered.

Deuterium signatures of CH_4 from sewage plants varied between −340.9 and −292.4‰, with an average of −303.9 ± 22‰ for the six UK sites, which is slightly more depleted in ^{2}H/H ratio compared to a US sewage treatment plant (−298‰) (Townsend-Small et al., 2016). A UK closed landfill site deuterium signatures (−269.9 ± 4‰) was similar to one active landfill site (−266.7 ± 1‰). These values are more enriched in comparison with the US active landfill, −290 ± 4‰ (Townsend-Small et al., 2016).

The isotopic signatures of CH_4 from the biogas plants and active landfills reveal greater ^{13}C depletions than CH_4 from other waste sources. The Net Zero Commission recommends that all biodegradable waste being sent to landfill sites in the UK will be banned within the next five years and more waste will be diverted to biogas and composting facilities (CCC, 2020). Therefore, isotopic signatures of waste emissions may change in coming years due to variation in waste management strategies. This study demonstrates that the unweighted and weighted averages of waste isotopic signatures are respectively −55.1 ± 4.1‰ and −56.1 ± 2.4‰. With the closure of active landfills but continued emissions from closed landfills and biogas plants, we can continue to use this isotopic range (−59.2 to −51‰) in the waste sector for the next few years.

4. Conclusion

This study focused on isotopic characterisation of CH_4 emission plumes from biogas plants, landfill sites, sewage treatment plants, water treatment plants, composting facilities and a leachate treatment plant in the UK, with additional sources measured in the Netherlands and Turkey. Overall, the $\delta^{13}C$-CH_4 and δ^2H-CH_4 signatures of biogas plants (−54.6 ± 5.6‰ n = 34; −314.4 ± 23‰ n = 3), landfills (−56.8 ± 2.3‰, n = 43; −268.2 ± 2.1‰, n = 2), sewage treatment plants (−51.6 ± 2.2‰, n = 15; −303.9 ± 22‰, n = 6), composting facilities (−54.7 ± 3.9‰, n = 6), landfill leachate treatment plants (−57.1 ± 1.8‰, n = 2), one water treatment plant (−53.7 ± 0.1‰) and one waste recycling centre (−53.2 ± 0.2‰) were assessed. These findings indicate how isotope signature of CH_4 from waste sources can differ within each category due to different input materials and processes.

$\delta^{13}C$ and δ^2H of CH_4 measured for air samples collected in plumes downwind of sources are in close agreement with those of previous studies for each source category, but extend the information to subdivide waste source categories by process. Our results highlight a clear isotopic distinction between active and closed landfill cells, as well as aerobic and anaerobic sewage treatment processes (Toyoda et al., 2011), which directly affect the emission source signature. Furthermore, differences in biogas feed-type influence the isotopic composition of the emitted CH_4, and this is tentatively related to the C4 and C3 vegetation types that are decomposing. These results can be applied to unmeasured sources across the UK in particular.

The most recent isotopic signature databases focus primarily on fossil fuel sources rather than biological sources, particularly waste sources (Milkov and Etiope, 2018; Sherwood et al., 2017). The new isotopic signature measurements are vital for closing the gap between CH_4 observations and isotopic inventories, which may understate waste sources like biogas plant emissions. This study isotopically characterised emissions from a total of 71 individual facilities, which contributes to the development of statistically more robust isotope signatures for non-fossil sources compared to the much larger fossil database and reduces uncertainties in the waste source signature. The findings can be used in atmospheric models to assess the impacts of waste CH_4 emissions and ongoing mitigation efforts. Our results extend those of Lowry et al. (2020), and Zazzeri at al. (2015) for UK CH_4 sources, but the new surveys specifically targeted waste sources, producing more detailed isotopic signature data.

Understanding the evolution of waste generation, the dominant source in a region and treatment processes can lead to the development of more effective mitigation strategies. The lack of integrated $\delta^{13}C$ and δ^2H data makes evaluating specific waste sources on a regional- and global-scale difficult. Also, long-term measurements of CH_4 mole fraction and isotopic signatures, combined with these findings, can be an effective tool for verifying emissions reductions, providing constraints for regional-scale inversion modelling and improving understanding of the $\delta^{13}C$ temporal trends of the global CH_4 record.

CRediT authorship contribution statement

Semra Bakkaloglu: Conceptualization, Methodology, Investigation, Formal analysis, Supervision, Validation, Writing – original draft, Writing – review & editing. **Dave Lowry:** Conceptualization, Methodology, Investigation, Supervision, Validation, Writing – review & editing. **Rebecca E. Fisher:** Conceptualization, Methodology, Investigation, Supervision, Validation, Writing – review & editing. **Malika Menoud:** Investigation, Methodology, Writing – review & editing. **Mathias Lanoisellé:** Methodology, Writing – review & editing. **Huilin Chen:** Investigation, Writing – review & editing. **Thomas Röckmann:** Investigation, Funding acquisition, Project administration, Writing – review & editing. **Euan G. Nisbet:** Conceptualization, Writing – review & editing.

Declaration of competing interest

The authors declare that they have no known competing financial interests or personal relationships that could have appeared to influence the work reported in this paper.

Acknowledgements

This work was supported by the MEthane goes MObile: MEasurement and MOdeling ($MEMO^2$) project, part of the European Union's Horizon 2020 research and innovation programme under Marie Sklodowska-Curie grant agreement No. 722479. We would like to thank the UK Natural Environment Research Council (NERC) for current grants: NE/P019641/1 New Methodologies for Removal of Methane and NE/N016238/1 The Global Methane Budget 2016–2021. We thank Jerry Morris for maintaining the survey vehicle, and James France for help with driving the vehicle for the surveys. Special thanks go to Mila Stanisavljevic, Sara Defratyka, Piotr Korben and Julianne Fernandez for sharing their $MEMO^2$ data, and colleagues in the Greenhouse Gas Research Group for supporting this study.

Appendix A. Supplementary data

Supplementary data to this article can be found online at https://doi.org/10.1016/j.atmosenv.2022.119021.

References

Akritas, M.G., Bershady, M.A., 1996. Linear regression for astronomical data with measurement errors and intrinsic scatter. Astrophys. J. 470, 706. https://doi.org/10.1086/177901.

Al-Shalan, A., Lowry, D., Fisher, R.E., Nisbet, E.G., Zazzeri, G., Al-Sarrawi, M., Fracne, J. L., 2022. Methane Emissions in Kuwait: plume identification, isotopic characterisation and inventory verification. Atmos. Environ. 268, 118763 https://doi.org/10.1016/j.atmosenv.2021.118763.

CCC, 2019. Net Zero Technical Report. Committee on Climate Change, London.

CCC, 2020. Reducing UK Emissions: 2020 Progress Report to Parliament. Committee on Climate Change, London.

Bakkaloglu, S., Lowry, D., Fisher, R.E., France, J.L., Brunner, D., Chen, H., Nisbet, E.G., 2021a. Quantification of methane emissions from UK biogas plants. Waste Manag. 124, 82–93. https://doi.org/10.1016/j.wasman.2021.01.011.

Bakkaloglu, S., Lowry, D., Fisher, R.E., France, J.L., Nisbet, E.G., 2021b. Carbon isotopic characterisation and oxidation of UK landfill methane emissions by atmospheric measurements. Waste Manag. 132, 162–175. https://doi.org/10.1016/j.atmosenv.2022.119021.

Beck, V., Chen, H., Gerbig, C., Bergamaschi, P., Bruhwiler, L., Houweling, S., Röckmann, T., Kolle, O., Steinbach, J., Koch, T., Sapart, C.J., 2012. Methane airborne measurements and comparison to global models during BARCA. J. Geophys. Res. Atmos. 117 (D15).

Bergamaschi, P., Lubina, C., Konigstedt, R., Fischer, H., Veltkamp, A.C., Zwaagstra, O., 1998. Stable isotopic signatures (delta C^{13}, delta D) of methane from European landfill sites. J. Geophys. Res. Atmos. 103, 8251–8265. https://doi.org/10.1029/98JD00105.

Börjesson, G., Samuelsson, J., Chanton, J., 2007. Methane oxidation in Swedish landfills quantified with the stable carbon isotope technique in combination with an optical method for emitted methane. Environ. Sci. Technol. 41, 6684–6690. https://doi.org/10.1021/es062735v.

Bousquet, P., Ciais, P., Miller, J.B., Dlugokencky, E.J., Hauglustaine, D.A., Prigent, C., Van der Werf, G.R., Peylin, P., Brunke, E.-G., Carouge, C., Langenfelds, R.L., Lathière, J., Papa, F., Ramonet, M., Schmidt, M., Steele, L.P., Tyler, S.C., White, J., 2006. Contribution of anthropogenic and natural sources to atmospheric methane variability. Nature 443, 439–443. https://doi.org/10.1038/nature05132.

Brass, M., Röckmann, T., 2010. Continuous-flow isotope ratio mass spectrometry method for carbon and hydrogen isotope measurements on atmospheric methane. Atmos. Meas. Tech. 10, 1707–1721. https://doi.org/10.5194/amt-3-1707-2010.

Dlugokencky, E.J., Bruhwiler, L., White, J.W.C., Emmons, L.K., Novelli, P.C., Montzka, S. A., Masarie, K.A., Lang, P.M., Crotwell, A.M., Miller, J.B., Gatti, L.V., 2009. Observational constraints on recent increases in the atmospheric CH_4 burden. Geophys. Res. Lett. 36 (18) https://doi.org/10.1029/2009GL039780.

Dlugokencky, E.J., Nisbet, E.G., Fisher, R., Lowry, D., 2011. Global atmospheric methane: budget, changes and dangers. Philos. Trans. Roy. Soc. A 369, 2058–2072. https://doi.org/10.1098/rsta.2010.0341.

EEA, 2020. Annual European Union Greenhouse Gas Inventory 1990–2018 and Inventory Report 2020. European Environment Agency, Copenhagen, Denmark. https://www.eea.europa.eu/publications/european-union-greenhouse-gas-inventory-2020.

Etminan, M., Myhre, G., Highwood, E.J., Shine, K.P., 2016. Radiative forcing of carbon dioxide, methane, and nitrous oxide: a significant revision of the methane radiative forcing. Geophys. Res. Lett. 43, 12614–12623. https://doi.org/10.1002/2016GL071930.

Fisher, R., Lowry, D., Wilkin, O., Sriskantharajah, S., Nisbet, E.G., 2006. High-precision, automated stable isotope analysis of atmospheric methane and carbon dioxide using continuous-flow isotope-ratio mass spectrometry. Rapid Commun. Mass Spectrom. 20, 200–208. https://doi.org/10.1002/rcm.2300.

France, J.L., Cain, M., Fisher, R.E., Lowry, D., Allen, G., O'Shea, S.J., Illingworth, S., Pyle, J., Warwick, N., Jones, B.T., Gallagher, M.W., Bower, K., Le Breton, M., Percival, C., Muller, J., Welpott, A., Bauguitte, S., George, C., Hayman, G.D., Manning, A.J., Lund Myhre, C., Lanoisellé, M., Nisbet, E.G., 2016. Measurements of δ13C in CH_4 and using particle dispersion modeling to characterize sources of arctic methane within an air mass. J. Geophys. Res. 121, 14257–14270. https://doi.org/10.1002/2016JD026006.

Hitchman, S.P., Darling, W.G., Williams, G.M., 1990. Stable isotope ratios in methane containing gases in the United Kingdom. British Geological Survey Technical Report WE89/30.

Hoheisel, A., Yeman, C., Dinger, F., Eckhardt, H., Schmidt, M., 2019. An improved method for mobile characterisation of delta (CH_4)-C-13 source signatures and its application in Germany. Atmos. Meas. Tech. 12, 1123–1139. https://doi.org/10.5194/amt-12-1123-2019.

Keeling, C.D., 1958. The concentration and isotopic abundances of atmospheric carbon dioxide in rural areas. Geochem. Cosmochim. Acta 13, 322–334. https://doi.org/10.1016/0016-7037(58)90033-4.

Lan, X., Basu, S., Schwietzke, S., Bruhwiler, L.M.P., Dlugokencky, E.J., Michel, S.E., Sherwood, O.A., Tans, P.P., Thoning, K., Etiope, G., Zhuang, Q., 2021. Improved constraints on global methane emissions and sinks using δ13C-CH4. Global Biogeochem. Cycles 35 (6), e2021GB007000.

Lassey, K.R., Allan, W., Fletcher, S.M., 2011. Seasonal inter-relationships in atmospheric methane and companion δ13C values: effects of sinks and sources. Tellus B 63, 287–301. https://doi.org/10.1111/j.1600-0889.2011.00535.x.

Levin, I., Bergamaschi, P., Dorr, H., Trapp, D., 1993. Stable isotopic signature of methane from major sources in Germany. Chemosphere 26, 161–177. https://doi.org/10.1016/0045-6535(93)90419-6.

Levin, I., Glatzel-Mattheier, H., Marik, T., Cuntz, M., Schmidt, M., Worthy, D.E., 1999. Verification of German methane emission inventories and their recent changes based on atmospheric observations. J. Geophys. Res. Atmos. 104, 3447–3456. https://doi.org/10.1029/1998JD100064.

Liptay, K., Chanton, J., Czepiel, P., Mosher, B., 1998. Use of stable isotopes to determine methane oxidation in landfill cover soils. J. Geophys. Res. Atmos. 103, 8243–8250. https://doi.org/10.1029/97JD02630.

Lopez, M., Sherwood, O.A., Dlugokencky, E.J., Kessler, R., Giroux, L., Worthy, D.E.J., 2017. Isotopic signatures of anthropogenic CH_4 sources in Alberta, Canada. Atmos. Environ. 164, 280–288. https://doi.org/10.1016/j.atmosenv.2017.06.021.

Lowry, D., Holmes, C.W., Rata, N.D., O'Brien, P., Nisbet, E.G., 2001. London methane emissions: use of diurnal changes in concentration and δ13C to identify urban sources and verify inventories. J. Geophys. Res. Atmos. 106, 7427–7448. https://doi.org/10.1029/2000JD900601.

Lowry, D., Fisher, R.E., France, J.L., Coleman, M., Lanoisellé, M., Zazzeri, G., Nisbet, E. G., Shaw, J.T., Allen, G., Pitt, J., Ward, R.S., 2020. Environmental baseline monitoring for shale gas development in the UK: identification and geochemical characterisation of local source emissions of methane to atmosphere. Sci. Total Environ. 708, 134600 https://doi.org/10.1016/j.scitotenv.2019.134600.

Lu, X., Harris, S.J., Fisher, R.E., France, J.L., Nisbet, E.G., Lowry, D., Röckmann, T., van der Veen, C., Menoud, M., Schwietzke, S., Kelly, B.F., 2021. Isotopic signatures of major methane sources in the coal seam gas fields and adjacent agricultural districts, Queensland, Australia. Atmos. Chem. Phys. Discuss. 1–36. https://doi.org/10.5194/acp-21-10527-2021.

Menoud, M., Röckmann, T., Fernandez, J., Bakkaloglu, S., Lowry, D., Korben, P., Schmidt, M., Stanisavljevic, M., Necki, J., Defratyka, S., Kwork, C.Y.a., 2020. Mamenoud/MEMO2_isotopes: v8.1 Complete. https://doi.org/10.5281/zenodo.4062356 [website]. (Accessed November 2020). Accessed on.

Menoud, M., van der Veen, C., Scheeren, B., Chen, H., Szénási, B., Morales, R.P., Pison, I., Bousquet, P., Brunner, D., Röckmann, T., 2020b. Characterisation of methane sources in Lutjewad, The Netherlands, using quasi-continuous isotopic composition measurements. Tellus B 72 (1), 1–20. https://doi.org/10.1080/16000889.2020.1823733.

Milkov, A.V., Etiope, G., 2018. Revised genetic diagrams for natural gases based on a global dataset of >20,000 samples. Org. Geochem. 125, 109–120. https://doi.org/10.1016/j.orggeochem.2018.09.002.

Monteil, G.A., Houweling, S., Dlugockenky, E.J., Maenhout, G., Vaughn, B.H., White, J. W.C., Rockmann, T., 2011. Interpreting methane variations in the past two decades using measurements of CH_4 mixing ratio and isotopic composition. Atmos. Chem. Phys. 11, 9141–9153. https://doi.org/10.5194/acp-11-9141-2011.

NAEI, 2022. National Atmospheric Emissions Inventory in 2019. NAEI, London.

Nisbet, E.G., Dlugokencky, E.J., Manning, M.R., Lowry, D., Fisher, R.E., France, J.L., Michel, S.E., Miller, J.B., White, J.W.C., Vaughn, B., Bousquet, P., Pyle, J.A., Warwick, N.J., Cain, M., Brownlow, R., Zazzeri, G., Lanoiselle, M., Manning, A.C., Gloor, E., Worthy, D.E.J., Brunke, E.G., Labuschagne, C., Wolff, E.W., Ganesan, A.L., 2016. Rising atmospheric methane: 2007–2014 growth and isotopic shift. Global Biogeochem. Cycles 30, 1356–1370. https://doi.org/10.1002/2016gb005406.

Nisbet, E.G., Manning, M.R., Dlugokencky, E.J., Fisher, R.E., Lowry, D., Michel, S.E., Myhre, C.L., Platt, S.M., Allen, G., Bousquet, P., Brownlow, R., 2019. Very strong atmospheric methane growth in the 4 years 2014–2017: implications for the Paris Agreement. Global Biogeochem. Cycles 33, 318–342. https://doi.org/10.1029/2018GB006009.

Nisbet, E.G., Dlugokencky, E.J., Fisher, R.E., France, J.L., Lowry, D., Manning, M.R., Michel, S.E., Warwick, N.J., 2021. Atmospheric methane and nitrous oxide: challenges along the path to Net Zero. Philos. Trans. Roy. Soc. A 379 (2210), 20200457. https://doi.org/10.1098/rsta.2020.0457.

NNFCC, 2021. Biogas map. Anaerobic Digestion [website]. http://www.biogas-info.co.uk/resources/biogas-map/.

Pataki, D.E., Bowling, D.R., Ehleringer, J.R., 2003. Seasonal cycle of carbon dioxide and its isotopic composition in an urban atmosphere: anthropogenic and biogenic effects. J. Geophys. Res. 108, 4735. https://doi.org/10.1029/2003JD003865.

Phillips, N.G., Ackley, R., Crosson, E.R., Down, A., Hutyra, L.R., Brondfield, M., Karr, D. J., Zhao, K., Jackson, R.B., 2013. Mapping urban pipeline leaks: methane leaks across Boston. Environ. Pollut. 173, 1–4. https://doi.org/10.1016/j.envpol.2012.11.003.

Polag, D., May, T., Müller, L., König, H., Jacobi, F., Laukenmann, S., Keppler, F., 2015. Online monitoring of stable carbon isotopes of methane in anaerobic digestion as a new tool for early warning of process instability. Bioresour. Technol. 197, 161–170. https://doi.org/10.1016/j.biortech.2015.08.058.

QGIS Development Team, 2021. QGIS geographic information system. Open Source Geospatial Foundation Project. http://qgis.osgeo.org.

Quay, P.D., King, S.L., Landsown, J.M., Wilbur, D.O., 1988. Isotopic composition of methane released from wetlands: implications for the increase in atmospheric methane. Global Biogeochem. Cycles 2, 285–397. https://doi.org/10.1029/GB002i004p00385.

Quay, P.D., King, S.L., Stutsman, J., Wilbur, D.O., Steele, L.P., Fung, I., Gammon, R.H., Brown, T.A., Farwell, G.W., Grootes, P.M., Schmidt, F.H., 1991. Carbon isotopic composition of atmospheric CH_4: fossil and biomass burning source strengths. Global Biogeochem. Cycles 5, 25–47. https://doi.org/10.1029/91GB00003.

Quay, P., Stutsman, J., Wilbur, D., Snover, A., Dlugokencky, E., Brown, T., 1999. The isotopic composition of atmospheric methane. Global Biogeochem. Cycles 13 (2), 445–461. https://doi.org/10.1029/1998GB900006.

Rice, A.L., Butenhoff, C.L., Teama, D.G., Röger, F.H., Khalil, M.A.K., Rasmussen, R.A., 2016. Atmospheric methane isotopic record favors fossil sources flat in 1980s and 1990s with recent increase. Proc. Natl. Acad. Sci. U.S.A. 113, 10791–10796. https://doi.org/10.1073/pnas.1522923113.

Rigby, M., Montzka, S.A., Prinn, R.G., White, J.W., Young, D., O'Doherty, S., Lunt, M.F., Ganesan, A.L., Manning, A.J., Simmonds, P.G., Salameh, P.K., Harth, C.M., Mühle, J., Weiss, R.F., Fraser, P.J., Steele, L.P., Krummel, P.B., McCulloch, A., Park, S., 2017. Role of atmospheric oxidation in recent methane growth. Proc. Natl. Acad. Sci. U.S.A. 114, 5373–5377. https://doi.org/10.1073/pnas.1616426114.

Röckmann, T., Eyer, S., Van der Veen, C., Popa, M.E., Tuzson, B., Monteil, G., Houweling, S., Harris, E., Brunner, D., Fischer, H., Zazzeri, G., Lowry, D., Nisbet, E. G., Brand, W.A., Necki, J.M., Emmenegger, L., Mohn, J., 2016. In situ observations of the isotopic composition of methane at the Cabauw tall tower site. Atmos. Chem. Phys. 16, 10469–10487. https://doi.org/10.5194/acp-16-10469-2016.

Saunois, M., Stavert, A.R., Poulter, B., Bousquet, P., Josep, G., Jackson, R.B., Raymond, P.A., et al., 2020. The global methane budget 2000–2017. Earth Syst. Sci. Data 12, 1561–1623. https://doi.org/10.5194/essd-12-1561-2020.

Schaefer, H., Fletcher, S.E.M., Veidt, C., Lassey, K.R., Brailsford, G.W., Bromley, T.M., Dlugokencky, E.J., Michel, S.E., Miller, J.B., Levin, I., Lowe, D.C., Martin, R.J., Vaughn, B.H., White, J.W.C., 2016. A 21st-century shift from fossil-fuel to biogenic methane emissions indicated by $13CH_4$. Science 352 (6281), 80–84. https://doi.org/10.1126/science.aad2705.

Schoell, M., 1980. The hydrogen and carbon isotopic composition of methane from natural gases of various origins. Geochem. Cosmochim. Acta 44, 649–661. https://doi.org/10.1016/0016-7037(80)90155-6.

Sherwood, O.A., Schwietzke, S., Arling, V.A., Etiope, G., 2017. Global inventory of gas geochemistry data from fossil fuel, microbial and burning sources, version 2017. Earth Syst. Sci. Data 9, 639–656. https://doi.org/10.5194/essd-9-639-2017.

Townsend-Small, A., Botner, E.C., Jimenez, K.L., Schroeder, J.R., Blake, N.J., Meinardi, S., Blake, D.R., Sive, B.C., Bon, D., Crawford, J.H., Pfister, G., 2016. Using stable isotopes of hydrogen to quantify biogenic and thermogenic atmospheric methane sources: a case study from the Colorado Front Range. Geophys. Res. Lett. 11, 462–471. https://doi.org/10.1002/2016GL071438, 11.

Townsend-Small, A., Tyler, S.C., Pataki, D.E., Xu, X., Christensen, L.E., 2012. Isotopic measurements of atmospheric methane in Los Angeles, California, USA: influence of

"fugitive" fossil fuel emissions. J. Geophys. Res. Atmos. 117 (D7) https://doi.org/10.1029/2011JD016826.

Toyoda, S., Suzuki, Y., Hattori, S., Yamada, K., Fujii, A., Yoshida, N., Kouno, R., Murayama, K., Shiomi, H., 2011. Isotopomer analysis of production and consumption mechanisms of N_2O and CH_4 in an advanced wastewater treatment system. Environ. Sci. Technol. 45, 917–922. https://doi.org/10.1021/es102985u.

Turner, A.J., Frankenberg, C., Wennberg, P.O., Jacob, D.J., 2017. Ambiguity in the causes for decadal trends in atmospheric methane and hydroxyl. Proc. Natl. Acad. Sci. U.S.A. 114, 5367–5372. https://doi.org/10.1073/pnas.1616020114.

Umezawa, T., Brenninkmeijer, C.A., Röckmann, T., Veen, C.V.D., Tyler, S.C., Fujita, R., Morimoto, S., Aoki, S., Sowers, T., Schmitt, J., Bock, M., 2018. Interlaboratory comparison of δ13C and δD measurements of atmospheric CH_4 for combined use of data sets from different laboratories. Atmos. Meas. Tech. 11 (2), 1207–1231. https://doi.org/10.5194/amt-11-1207-2018.

UNFCCC, 2017. United Nations Framework Convention on Climate Change, 2017. Methodological Tool, Project and Leakage Emissions from Anaerobic Digestion. Geneva, Switzerland.

Wang, J., Zhang, J., Xie, H., Qi, P., Ren, Y., Hu, Z., 2011. Methane emissions from a full-scale A/A/O wastewater treatment plant. Bioresour. Technol. 102 (9), 5479–5485. https://doi.org/10.1016/j.biortech.2010.10.090.

White, J.W.C., Vaughn, B.H., Michel, S.E., 2017. Stable Isotopic Composition of Atmospheric Methane (13C) from the NOAA ESRL Carbon Cycle Cooperative Global Air Sampling Network, 1998–2015. Version: 2017-01-20, available at:. University of Colorado, Institute of Arctic and Alpine Research (INSTAAR). last access: ftp://aftp.cmdl.noaa.gov/data/trace_gases/ch4c13/flask/. (Accessed 28 August 2017).

Whiticar, M.J., 1990. A geochemical perspective of natural gas and atmospheric methane. Org. Geochem. 16, 531–547. https://doi.org/10.1016/0146-6380(90)90068-B.

Whiticar, M.J., 1999. Carbon and hydrogen isotope systematics of bacterial formation and oxidation of methane. Chem. Geol. 161 (1–3), 291–314.

Worden, J.R., Bloom, A.A., Pandey, S., Jiang, Z., Worden, H.M., Walker, T.W., Houweling, S., Röckmann, T., 2017. Reduced biomass burning emissions reconcile conflicting estimates of the post-2006 atmospheric methane budget. Nat. Commun. 8 (1), 1–11.

Xueref-Remy, I., Zazzeri, G., Bréon, F.M., Vogel, F., Ciais, P., Lowry, D., Nisbet, E.G., 2020. Anthropogenic methane plume detection from point sources in the Paris megacity area and characterization of their δ13C signature. Atmos. Environ. 222, 117055 https://doi.org/10.1016/j.atmosenv.2019.117055.

Yang, S., Lan, X., Talbot, R., Liu, L., 2019. Characterizing anthropogenic methane sources in the Houston and Barnett Shale areas of Texas using the isotopic signature δ13C in CH_4. Sci. Total Environ. 696, 133856 https://doi.org/10.1016/j.scitotenv.2019.133856.

Zazzeri, G., Lowry, D., Fisher, R.E., France, J.L., Lanoisellé, M., Nisbet, E.G., 2015. Plume mapping and isotopic characterisation of anthropogenic methane sources. Atmos. Environ. 110, 151–162. https://doi.org/10.1016/j.atmosenv.2015.03.029.

Zazzeri, G., Lowry, D., Fisher, R.E., France, J.L., Lanoisellé, M., Kelly, B.F.J., Necki, J.M., Iverach, C.P., Ginty, E., Zimnoch, M., Jasek, S., Nisbet, E.G., 2016. Carbon isotopic signature of coal-derived methane emissions to the atmosphere: from coalification to alteration. Atmos. Chem. Phys. 16, 13669–13680. https://doi.org/10.5194/acp-16-13669-2016.

Zazzeri, G., Lowry, D., Fisher, R.E., France, J.L., Lanoisellé, M., Grimmond, C.S.B., Nisbet, E.G., 2017. Evaluating methane inventories by isotopic analysis in the London region. Sci. Rep. 7, 1–13. https://doi.org/10.1038/s41598-017-04802-6.